6448 *Macromolecules* **2009**, *42*, 6448–6456
DOI: 10.1021/ma900952e

Macromolecules
ARTICLE

Can Nonspecific Host−Guest Interaction Lead to Highly Specific Encapsulation by a Supramolecular Nanocapsule?

Decheng Wan,* Guangcheng Wang, Hongting Pu, and Ming Jin

Institute of Functional Polymers, School of Materials Science and Engineering, Tongji University, 1239 Siping Road, Shanghai 200092, China

Received May 1, 2009; Revised Manuscript Received June 1, 2009

ABSTRACT: A general and facile approach for highly selective separation of ionic dyes is described. Core−shell amphiphilic macromolecular nanocapsule (CAM) derived from hyperbranched polymer is structurally featured by the dense functional groups populated in the core, which provide a unique opportunity for the core engineering and structure−property evaluation of a CAM. Here hyperbranched polyethylenimine (HPEI) is alkylated with 2-hexadecyloxymethyloxirane via a single-step, mild and efficient reaction, leading to HP(EI-C16$_x$) (x = 0.10 (**1a**), 0.15 (**1b**), 0.20 (**1c**), 0.30 (**1d**), 0.60 (**1e**), and 0.90 (**1f**), where x represents the fraction of amino protons being alkylated) with a hydrophobic shell and a hydrophilic core. The core of **1d** is further treated with propylene oxide, glycidol, methyl iodide, or succinic anhydride, respectively, leading to hydroxyls (**2d**, **3d**), quaternized ammoniums (**4d**) and carboxyls (**5d**) populated core. These CAMs show different guest loading capacity and guest recognizing ability and can be used for highly selective separation of water-soluble ionic dyes. For example, **1a**−**1e** can 100% separate cationic−anionic dyes and some anionic−anionic dyes; **4d** shows the highest encapsulating capacity and can encapsulate a broad spectrum of guests but with a relatively low selectivity; **1f** and **2d** can recognize broader spectrum of guests and can ∼100% separate various binary anionic dyes and some ternary anionic dyes. These CAMs can recognize not only anionic dyes bearing different charges but also those bearing the same number of ionic charge(s). These results indicate that for a host−guest system mainly based on nonspecific interaction, highly specific encapsulation can be a general case because accumulated multisite statistical host−guest interaction can differentiate the guests, where the core of the CAM plays a crucial role in guest recognition.

Introduction

Supramolecular host−guest chemistry has caused much interest in recent years,[1] but the guest selectivity is still a central issue. The host−guest interaction can be roughly divided into two kinds in terms of selectivity, one is based on specific interaction such as multiple hydrogen-bonding interaction where high selectivity is generally found due to specificity, cooperativity, directionality, and saturable nature of such interaction, and the selectivity can be enhanced by combining with topological trapping;[2] the other is based on nonspecific interaction such as ionic interaction, hydrophobic interaction where the selectivity is still a general concern. Although highly selective entrapping of ionic sodium and potassium by crown ether is well-known,[3] the selectivity stems mainly from the topological and metal−ligand factor rather than from electrostatic factor.

In the recent decade, CAM derived from hyperbranched polymer[4] becomes very popular for the cost-effective production, wide availability and versatile guest encapsulation,[5−20] but high selectivity on encapsulation of ionic guests has rarely been reported.[20−23] Unlike a dendrimer with well-defined structure and regularly arrayed active sites on the periphery,[24] hyperbranched polymer is asymmetric in structure and the functional groups randomly distribute core through shell. On the other hand, nonspecific host−guest interaction is based on statistical accumulation of host−guest complementary interaction in all aspects, where comprehensive guest recognition is theoretically possible if tailoring a host according to the guest is feasible. In this regard, CAM derived from hyperbranched polymer is advantageous because the residual functional groups in the core can provide a unique opportunity for the core engineering.[22] We showed previously that the core engineering of a CAM could lead to 100% separation of anionic−cationic guest mixture, but the separation of anionic−anionic dyes was relatively limited, for example, methyl orange (MO)/ Rose Bengal (RB) could not be highly efficiently separated.[21] Now several issues need clarifying: (1) why can some guests be encapsulated, while others cannot be; (2) can complete separation of anionic guests be possible and be a general case (?) where challenge mainly stems from the nonspecific nature of host−guest interaction; (3) loading two or more guests in one CAM at a predetermined ratio is sometimes desired, but is this possible and what factor determines the ratio? Here in this article, CAMs with a thicker shell than previous ones are synthesized with meticulously tailored cores, and their guest affinity, guest recognition ability, and guest loading capacity are studied, and facile 100% or nearly 100% separation of binary and ternary anionic guests is reported as a general case for the first time, where the nature of functional sites in the core playing a critical role.

Results and Discussion

A. Synthesis of CAMs. The CAMs reported here are similar to previous ones[21,22] but with a thicker hydrophobic shell. The synthesis of CAMs with different shell density (degree of functionalization) is outlined in Scheme 1 and the core engineering of one CAM is outlined in Scheme 2. 2-hexadecyloxymethyloxirane is synthesized via phase transfer catalytic Williamson reaction of epichlorohydrin with

*Corresponding author. E-mail: wandecheng@tongji.edu.cn. Fax: ++86 21 65982461.

 Published on Web 06/26/2009

Scheme 1. Outline of the Synthesis of CAM 1a−f, Wherein *x* Represents the Fraction of Amino Protons Being Alkylated[a]

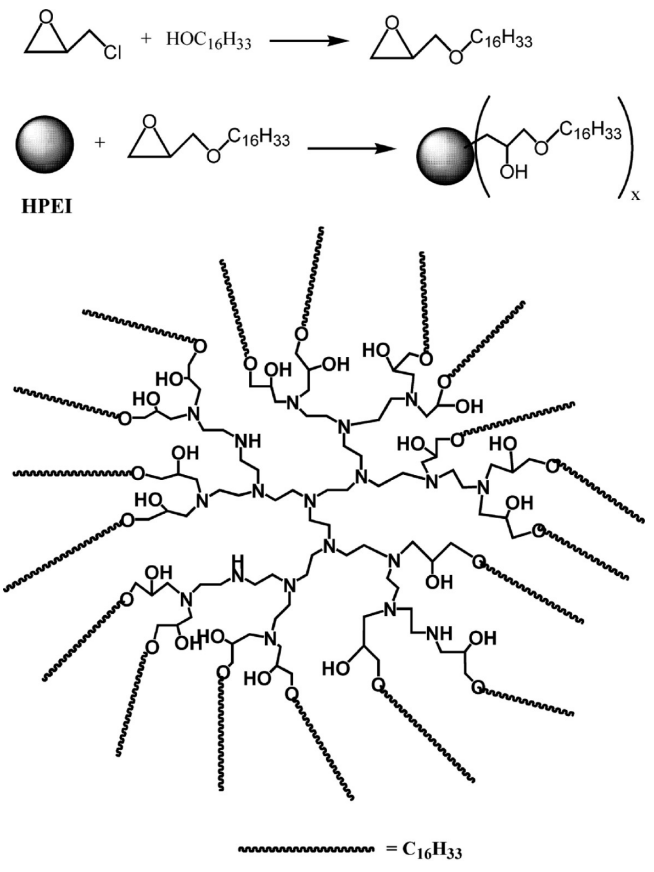

x = 0.10 (**1a**); 0.15 (**1b**); 0.20 (**1c**); 0.30 (**1d**); 0.60 (**1e**); 0.90 (**1f**)

[a] HPEI has 232 repeat units but only 17 of them are shown here for clarity.

1-hexadecanol, the resulting product reacts efficiently with HPEI under a mild condition, leading to HP(EI-C16$_x$) (x = 0.10 (**1a**), 0.15 (**1b**), 0.20 (**1c**), 0.30 (**1d**), 0.60 (**1e**), 0.90 (**1f**)) with different shell density and also different core. Figure 1 shows the ^{1}H NMR spectrum of 2-hexadecyloxymethyloxirane, where all expected proton signal appears and the signal intensity agrees well with the expected number of protons, the signals of proton g and e are split due to the presence of a chiral carbon.

Figure 2 shows the ^{1}H and ^{13}C NMR of **1d**, where all the signals appear and the signal intensity agrees well with the expected structure, but a signal around 3.65 ppm also appears, whose intensity is random (figure 3) and should be attributed to an impurity. From the ^{1}H NMR spectrum, it can be derived that 30% of the amino protons are alkylated by the epoxy group, the same as in the feed ratio. Dialysis in chloroform for 24 h leads to no difference in spectrum or loss of the mass. From the mass increase, it also can be derived that the reaction efficiency is ~100%. But for **1f**, excess 2-hexadecyloxymethyloxirane is used and dialysis is necessary to remove the reactant in excess. Figure 3 shows the ^{1}H NMR spectra of **1a**−**f**.

From Figure 3, the molecular weight of each CAM can be derived, and the results are collected in Table 1. **2d**, **4d**, and **5d** are synthesized according to the synthesis of similar compounds[22] and are purified by dialysis against chloroform. **3d** are synthesized similar to **2d**. Figure 4 shows the ^{1}H NMR spectra of **3d** and **4d**, and their molecular weights derived from ^{1}H NMR are also collected in table 1. CAM **1a**−**f** are with a thicker shell and are solids, in contrast to the liquid form of previously reported CAM with a thinner shell. CAM **1a**−**f** are soluble in a broad range of solvents, as shown in table 2. It can be found from Table 2 that CAMs with medium shell density are soluble in a broader range of solvents such as ethanol, ether, and *n*-hexane, as compared with those bearing low or high shell density. It is known that the guest loading capacity of a CAM is greatly dependent on its physical state because the aggregate and unimolecular micelle (UIM[1a]) show rather different encapsulating capacity,[10,14,15,21,22] thus the aggregation behavior of the CAMs are measured at a specified concentration of 1×10^{-6} M, at which most of the encapsulating experiments are carried out, and the aggregation results are collected in Table 1. It can be found from Table 1 that most of the CAMs exist in the form of aggregate but the CAMs with charged core (**4d**) or with the densest shell (**1f**) exist in the form of UIM. It will be found later that though the aggregate influences the encapsulating capacity, it exerts little influence on the guest affinity, and either the aggregate or the UIM can encapsulate guests.

B. Guest Encapsulation by CAMs. *1. Role of the Core on Guest Loading Capacity*. All of the CAMs bear a polar core which can interact with hydrophilic guests, and bear a hydrophobic shell which renders them soluble in a variety of apolar organic solvents. It is found that anionic, water-soluble MO (Chart 1) in water can be transferred to organic phase by any of the CAMs via the liquid−liquid biphasic extraction. Experimentally, when MO is charged in a biphasic mixture of water/chloroform, the aqueous layer is colorized while the oil layer keeps colorless, but upon the addition of an appropriate amount of CAM under shaking, the organic layer is colorized while the aqueous layer becomes colorless, indicating the transferring of MO is due to the CAM. Figure 5 shows the transfer of MOs to oil by a stock solution of **1d**, **2d**, or **3d** as a function of MO concentration. All the phase transfer behavior shows a 2-stage character within the tested range, during stage 1, the MOs are completely transferred to oil, while during stage 2, only part of the MOs are transferred. From the inflection point, the MOs encapsulated by each CAM can be derived and the results are collected in table 3, where those encapsulated by **4d** and **5d** are also shown.

It can be found from Table 3 that the core structure has great impact on the encapsulating capacity of the CAM, where a 38-fold difference is observed among the CAMs with different core. **4d** shows the highest capacity for the complementary anionic−cationic host−guest interaction. Among the five CAMs of **1d**−**5d**, the core of **1d** is relatively hydrophobic, and **1d** shows the second highest capacity because the MO is also relatively hydrophobic; for **2d**, the alkylation of amines leads to a core more susceptible to protonation by water, thus cationic−anionic interaction should be enhanced, but a much suppressed encapsulating ability is observed, a similar behavior is found for **3d**. This behavior can be attributed to two factors, one is the produced hydroxyl groups that are polar and unfavorable for the accommodation of MO, the other is the alkylating groups which occupy part of the room that could be provided for the guest. **5d** shows the lowest encapsulating ability because the anionic carboxyl groups in the core confer ionic repulsion toward the anionic guest. One may argue that **4d** is a UIM while the other CAMs are aggregate thus the difference can be at least partly attributed to the aggregation. To probe the reason, the encapsulating capacity of **1f** is also measured, and the value is 17.5. One can find that both **1f** and **4d** are in the form of UIM, but they show a great difference in

loading capacity. These results strongly suggest that the chemically different core is mainly responsible for the guest loading capacity.

2. Role of the Core on Cationic−Anionic Guest Separation. It is found that any cationic−anionic pair of ionic dyes listed in Chart 1 can be 100% separated by any CAM but **4d**. Experimentally, CAM in chloroform (generally at 1×10^{-6} M) is added in a titration-like manner to a pair of dyes in biphasic mixture of water/chloroform with shaking, when the amount of CAM is higher than a critical value, the mixed dyes can be completely separated into two phases: the cationic MB in water and the anionic dye in oil. With more CAM added into the system, the cationic MB cannot be transferred into the oil phase. In further tests, only a single dye MB is tested, no MB can be encapsulated, moreover, the existence of MB in the system does not exert any influence on the encapsulating capacity of CAM to another dye. It is worth to notice that though any of the dye alone is insoluble in chloroform, some of the cationic−anionic mixtures (the pair of MO/MB and RB/MB) are soluble in chloroform even without CAM, which should originate from the ionic neutralization of the oppositely charged guests (the ionic neutralization generally leads to enhanced hydrophobicity, but the CR is very hydrophilic that the neutralization does not lead to any oil solubility, while for the pair MeB/MB, precipitation occurs), but upon the addition of the CAMs, the anionic dyes reside in the oil layer while the cationic MB return to the water phase, most probably because the anionic dyes are encapsulated and thus ionic neutralization can no longer occur. Among the CAMs, **4d** is the only CAM that can encapsulate cationic MB, thus is not recommended for the separation of cationic−anionic mixture. That **4d** can encapsulate MB indicates the polarity of the core plays an important role in guest encapsulation. This experiment also shows that the core engineering can lead to the encapsulation of broader spectrum of guests.

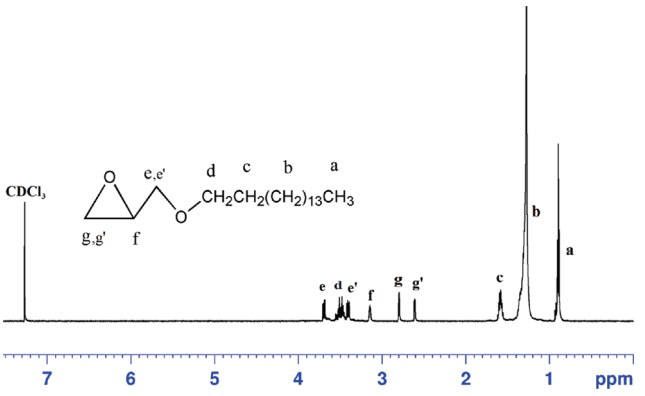

Figure 1. ^{1}H NMR of 2-hexadecyloxymethyloxiane ($CDCl_3$).

3. Role of the Core on Anionic−Anionic Guest Separation. Although the separation of anionic−cationic dyes with the aid of CAM is relatively easy, the separation of anionic ones is much more difficult. However, with the core engineering, effective recognition of anionic guests is found. Figure 6

Scheme 2. Outline of the Synthesis of 2d−5d by Core Engineering of 1d

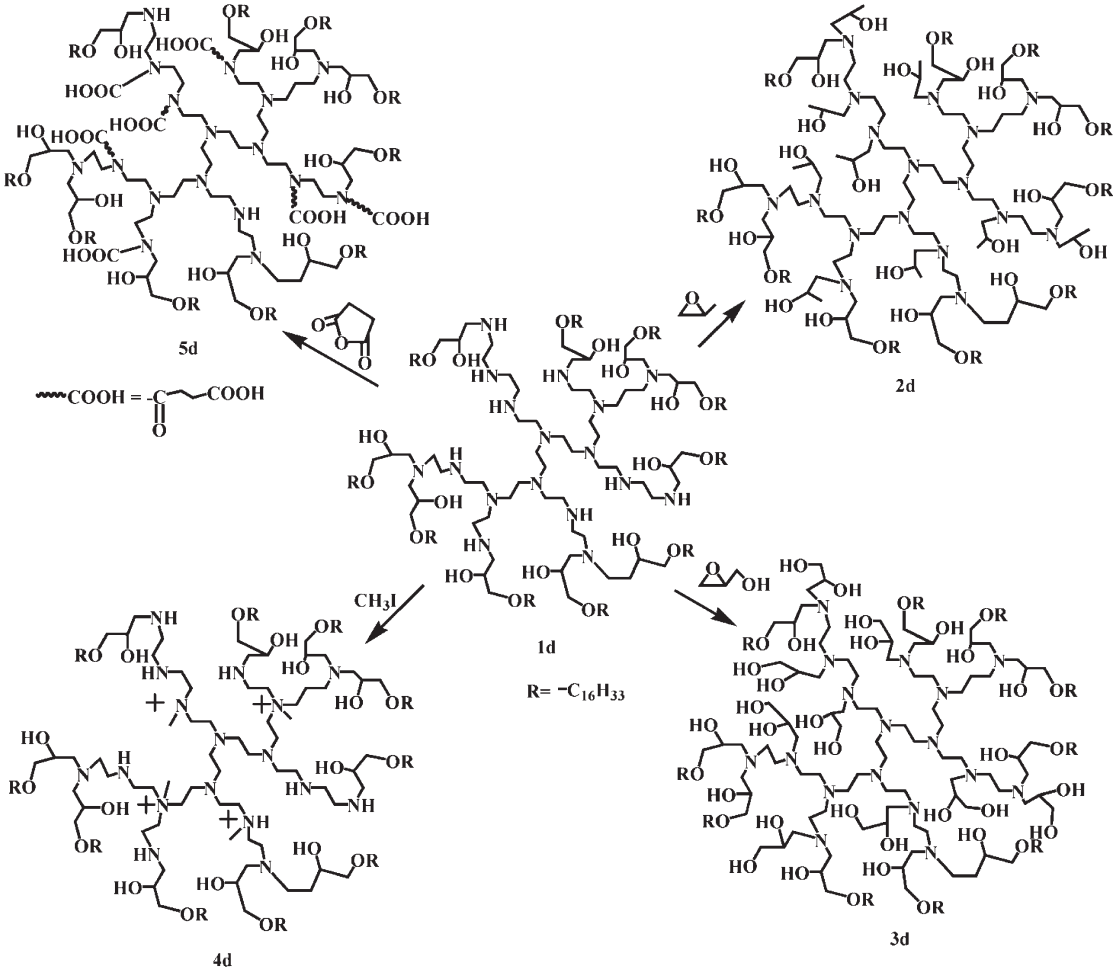

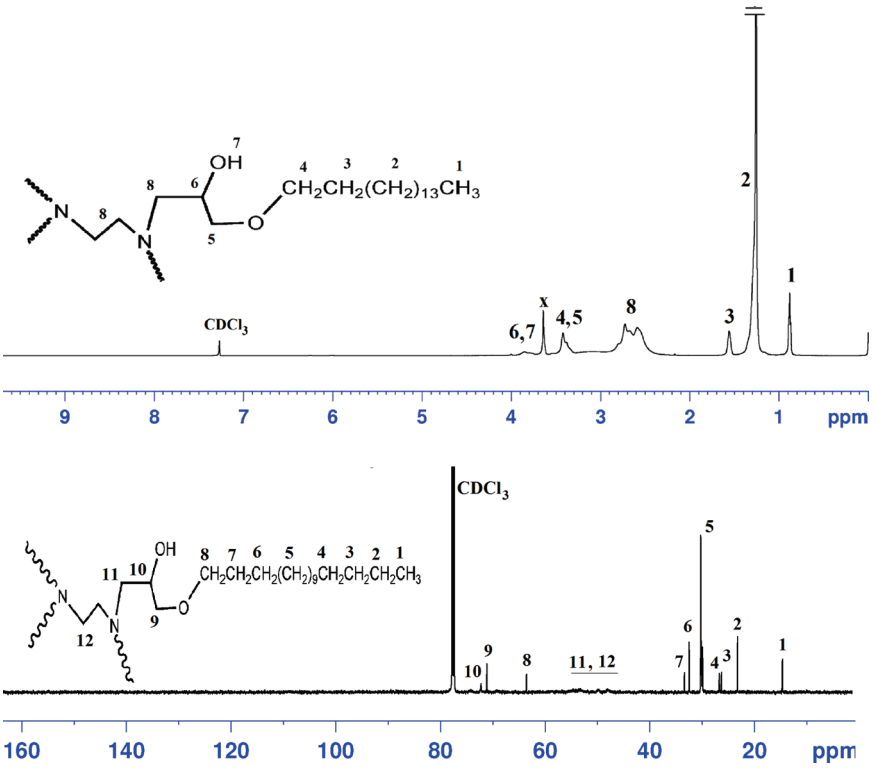

Figure 2. ^{1}H and ^{13}C NMR of **1d** ($CDCl_3$) (x represents an impurity).

shows that the mixture of anionic MeB and RB can be highly selectively distinguished by CAM **1a**−**1f** and **2d** which are in the form of an aggregate at 1×10^{-6} M. Experimentally, the CAM in chloroform (1×10^{-6} M) is added to the aqueous MeB/RB mixture with shaking, and the addition is continued until no RB can be detected in the aqueous phase. UV/vis spectra analysis shows only RB moves into the oil phase, even much excess CAM is used, no MeB can be detected in the oil, indicating the CAM can effectively recognize this pair of anionic guests. The mixture of anionic MO/MeB is tested similarly and the separation is also 100% as that of MeB/RB, as measured by UV/vis spectra. In further tests, only the single dye of MeB is tested, and it is found that none of **1a**−**1f** and **2d** (at 1×10^{-6} M) can encapsulate any MeB. Interestingly, Gao et al.[11] reported previously a 40—100-fold synergic encapsulation of MeB with the aid of MO in case of their CAMs. In our system, no synergic effect is found and 100% separation of MO/MeB is found, which we believe should be attributed to the difference in the core of these CAMs.

Among the CAMs, **4d** exists as UIM at 1×10^{-6} M, and shows the highest encapsulating capacity and also can encapsulate the widest spectrum of guests, but is rather limited in guest recognition. The only pair of binary anionic mixture that can be separated by **4d** is RB/MeB, figure 7 shows that RB/MeB is nearly 100% separated with an appropriate amount of **4d**, the encapsulating capacity is 22 RBs/**4d**. For comparison, single-dye encapsulation is also carried out, with 1.1 MeBs/**4d** and 22 RBs/**4d** being found, indicating the presence of MeB does not interfere with the encapsulation of RB.

1a−**1d** are also employed to distinguish MO/RB, but show rather limited selectivity. Figure 8 shows the result, where both MO and RB are transferred to the oil phase. One thing we are interested in is what factor determines the ratio of MO/RB transferred to oil, the guest ratio or the CAM structure? Thus experiment is carried out at different guest ratios with different CAMs, table 4 shows the results. It can be found from Table 4 that the guest ratio transferred to the oil is mainly determined by the guest concentration in feed, but the structure of CAM also has some influence on the ratio. These results show that **1a**, **1b** shows rather limited guest selectivity on MO/RB, and to encapsulate MO/RB at an invariable predetermined ratio is not possible yet.

When **1e** is used in place of **1a**, the selectivity is greatly improved, further test with **1f** shows completely separation of MO from RB. Experimentally, to an aqueous mixture of MO/RB ([MO] + [RB] = 10^{-4} M), **1f** in chloroform (1×10^{-6} M) is added gradually with shaking, RB is preferentially transferred to the oil (5.5 RBs/**1f**), while in the absence of MO, the RBs transferred to the oil is also 5.5 RBs/**1f**, and if only MOs exist, it is 45 MOs/**1f**. Alternatively, certain amount of **1f** in chloroform is saturated with RB, followed by shaking with aqueous MO, when a phase balance is reached, the oil is separated and analyzed by UV/vis measurement, and hardly any RB is replaced by MO, as shown in Figure 9. This behavior is independent of the addition sequence of the dyes, indicating that the guest selection is due to the guest affinity of the core rather than the topological selectivity. In a previous report,[21] it was noticed that HP (EI-$C12_{0.86}$) could completely separate MO/CR but could not 100% separate MO/RB. In contrast, **1f** (HP(EI-$C16_{0.9}$)) can ~100% separate MO/RB, which should be attributed to higher alkylation of the core of **1f** because it has been shown that the shell thickness has little influence on the guest selectivity of a CAM.[22]

To further probe the guest selection mechanism, **1d** and **2d** are used in place of **1f** respectively, and it shows that **2d** leads to the same separation efficiency to **1f** while **1d** shows a poor selectivity. It is known that **2d** has a core that is almost the same as **1f** but the shell is different, while **1d** has the same shell as **2d** but the core is very different from that of **2d** and **1f**, thus the guest selectivity is due to the difference in core. Another concern is whether the aggregation exerts any influence on the encapsulating behavior because **1f** exists as UIM while

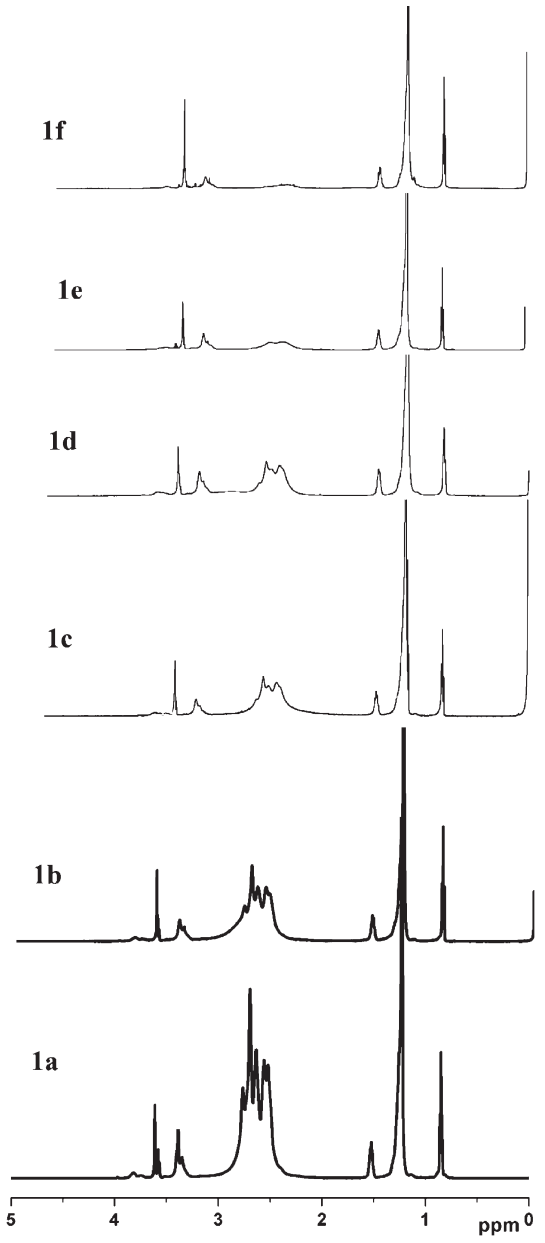

Figure 3. ^{1}H NMR spectra of **1a**−**f** ($CDCl_3$).

1a−**1e** and **2d** exist as aggregate, but since **1e**, **2d** (aggregate), and **1f** (UIM) show similar selecting behaviors, the selectivity seems to have no relation to the aggregation.

As pointed out previously, summation of multisite statistical interaction can amplify the host−guest binding strength;[22] thus, RB should bind stronger to the host than MO because RB bears two anionic charges while MO bears only one, and this may be the underlying factor for the selectivity. According to this hypothesis, MeB, which bears three anionic charges, should bind stronger to the CAM than RB and MO, however, none of **1a**−**1f**, **2d**, and **3d** can encapsulate MeB, which should be attributed to the strong hydrophilicity of MeB.

Up to now, any pair of anionic dyes in Chart 1 which bear different charges can be ∼100% separated, this can be mainly attributed to their anionic charges which bind to CAM at different strength. In this regards, the pair of RB/CR should be the most difficult to be separated because both bear two anionic charges. However, it is experimentally found that most of the CAMs can highly selectively separate

Table 1. Molecular Weight of 1a−f and 2d−5d Derived from ^{1}H NMR and Their Particle Size and Size Distribution in Chloroform

CAM	structure[a]	M_n	D_h/nm[b]	$\mu^2/\langle\Gamma\rangle^{2}$ [b]
1a	HP(EI-$C16_{0.1}$)	17200	166.6	0.59
1b	HP(EI-$C16_{0.15}$)	20800	155.6	0.63
1c	HP(EI-$C16_{0.2}$)	24400	104.4	0.31
1d	HP(EI-$C16_{0.3}$)	31600	53.0	0.31
1e	HP(EI-$C16_{0.6}$)	53300	41.0	0.2
1f	HP(EI-$C16_{0.9}$)	74900	9.0	0.19
2d	HP(EI-$C16_{0.3}PO_{0.7}$)	41000	87.9	0.45
3d	HP(EI-$C16_{0.3}GO_{0.7}$)	43600	114.4	0.51
4d	HP(EI-$C16_{0.3}N^{+}_{0.32})I^{-}$	42160	7.7	0.23
5d	HP(EI-$C16_{0.3}COOH_{0.4}$)	40880	139	0.61

[a] Nomenclature: for example HP(EI-$C16_{0.3}PO_{0.7}$) means 30% of the amino protons are alkylated with 2-hexadecyloxymethyloxirane and the residual 70% are alkylated with propylene oxide (PO); GO represents glycidol. [b] Measured at a specified concentration of 1×10^{-6} M. D_h: diameter of particle size. $\mu^2/\langle\Gamma\rangle^2$: polydispersity of the particle size.

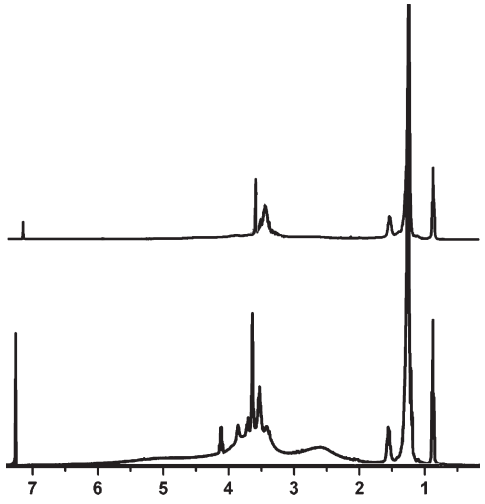

Figure 4. ^{1}H NMR of **3d** (bottom) and **4d** (up) in $CDCl_3$.

Table 2. Solubility of HP(EI-$C16_x$) (1a−f) in a Variety of Solvents[a]

	x	$CHCl_3$	toluene	THF	ether	acetone	EtOH	*n*-hexane
HPEI	0	○	×	×	×	×	○	×
1a	0.10	○	○	○	×	○	○	○
1b	0.15	○	○	○	○	○	○	○
1c	0.20	○	○	○	○	○	○	○
1d	0.30	○	○	○	○	○	○	○
1e	0.60	○	○	○	○	×	×	○
1f	0.90	○	○	×	×	×	×	×

[a] Tested at room temperature. Key: ○, soluble; ×, insoluble; THF, tetrahydrofuran; ether, diethyl ether; EtOH, ethanol.

RB/CR, figure 10 shows the result, where ∼100% separation of RB/CR by **1a**, **1b**, and **1d** are shown. In single-dye encapsulation, it is found that these CAMs are reluctant to encapsulate CR, and generally a precipitation will occur, which render the exact determination of encapsulating capacity difficult. Interestingly, in double-dye encapsulation, less precipitation is found. Most likely, the RB is relatively hydrophobic thus binds stronger to the CAM than CR does, and this reason can explain why **2d** is less efficient (for its more polar core) to separate them.

On the basis of the aforementioned result, the separation of ternary anionic mixture such as MO/RB/MeB is possible, as shown in Figure 11, where the CAM can be repeatedly reused because the guest can be released under the stimulus of high pH.

Chart 1. Structure of Several Ionic Dyes

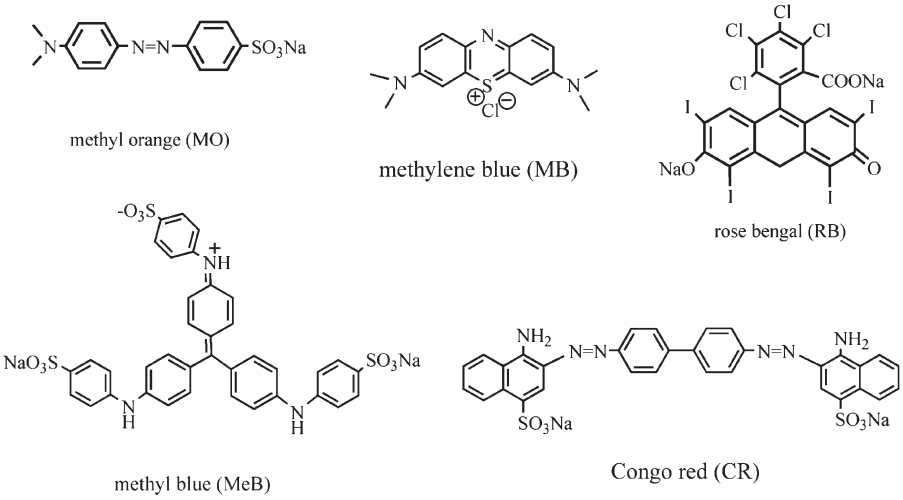

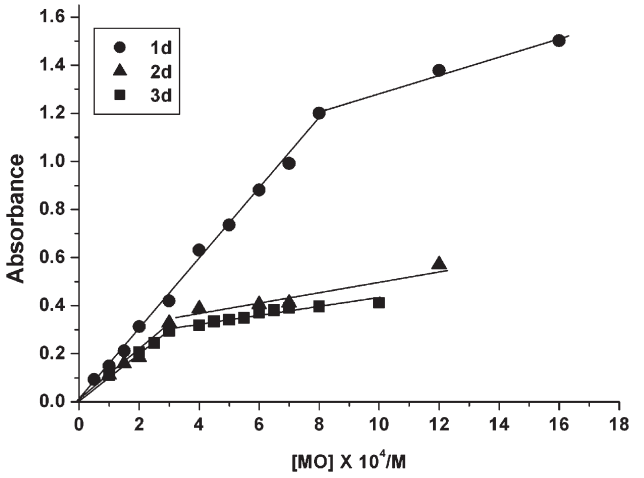

Figure 5. MOs transferred to the oil phase by a stock solution of CAM **1d**−**3d** as a function of aqueous MO concentration. Conditions: [CAM] = 1×10^{-6} M, [MO] = $(0.5-16)\times10^{-4}$ M.

Conclusion. We have shown here that for host−guest system based on nonspecific interaction, highly specific encapsulation can be a general case. All the tested anionic−cationic and anionic−anionic guest mixtures can be ~100% distinguished by a host CAM if the discrepancy among the guests is taken into account during the core engineering of the CAM. The separation is based on the principle that statistical accumulation of nonspecific interactions can amplify the host−guest binding strength and thus differentiate the guests. Such a CAM combines several merits in separation of ionic mixture: hydrolysis-resistance, pH-responsive release, high guest selectivity, repeatedly reusable property, and convenient separation operation. We also show that with the core engineering, the encapsulating capacity can be greatly improved, and a wider spectrum of guests can be encapsulated, and CAMs with different core show different performance in guest separation. We believe this discovery will be suggestive for other fields such as medical, nanoreactor and catalytic chemistry.

Experimental Section

Materials. Hyperbranched polyethylenimne (HPEI, $M_n = 1\times10^4$, $M_w/M_n = 2.5$, degree of branch (DB) = 60%,[9] Aldrich), glycidol (96%, Aldrich). Methyl orange (MO), methyl blue (MeB), Congo red (CR), Rose Bengal (RB), methylene blue (MB), propylene oxide, methyl iodide, 1-hexadecanol, epichlorohydrin, succinic anhydride, poly(ethylene oxide) ($M_n = 1100$, Fluka), KOH. All the chemicals were purchased from SCRC (China) with the highest purity available unless state otherwise, and are used directly.

Table 3. MOs Encapsulated by 1d-5d at the Inflection Point[a]

CAM	MOs encapsulated per CAM
1d	55
2d	16
3d	14
4d	139
5d	3.6
1f	17.5

[a] Liquid−liquid extraction of aqueous MO by a CAM in chloroform. See Figure 5 for the inflection point where the values are derived. [CAM] = 1×10^{-6} M.

Synthesis. *2-Hexadecyloxymethyloxirane (**HO**).* A mixture of epichlorohydin (52 g, 562 mmol), 1-hexadecanol (24.2 g, 100 mmol), KOH (18 g, 300 mmol) and poly(ethylene oxide) (2 g, $M_n = 1000$) was prepared and stirred at 50−60 °C for 2 days. The mixture was poured into a large amount of water with vigorous shaking. The mixture was extracted with chloroform (3×200 mL), the combined chloroform was washed with cold water. After the chloroform was removed on a rotary evaporator, the residue was dissolved in diethyl ether and the solution was washed again with cold water (2×150 mL) and finally dried over sodium sulfate. The organic was separated by filtration, removal of the volatile via rotary evaporator yielded a white solid (28.3 g, 95%). ^{1}H NMR (δ/ppm): 0.90 (t, 3H, CH_3), 1.28 (s, 26H, $OCH_2CH_2(CH_2)_{13}CH_3$), 1.57 (t, 2H, OCH_2CH_2), 3.66 (t, 2H, OCH_2CH_2), 3.13 (m, 1H, CH), 2.60, 2.80 (m, 2H, CH_2(O)CH), 3.48, 3.70 (m, 2H, CH_2(O)$CHCH_2OC_{16}H_{33}$).

*Synthesis of **1a**−**d**.* The synthesis is exemplified by the synthesis of **1d**. HPEI (1 g, equivalent of 23.2 mmol of NH) in ethanol (8 mL) was mixed with **HO** (2.07 g, 6.96 mmol), and the transparent mixture was stirred at room temperature for 3 days. After the solvents were removed on a rotary evaporator, a quantitative product (3.07 g) was obtained as a solid. Dialysis against chloroform (Spectro/Por, MWCO 2000) for 3 days led to no loss of the product.

*Synthesis of **1e**, **1f**.* The synthesis is exemplified by the synthesis of **1f**. HPEI (1.5 g, equivalent of 34.9 mmol of NH) in ethanol (10 mL) was mixed with **HO** (10.4 g, 35 mmol), and the transparent mixture was stirred at room temperature, after 1 day the mixture became opaque, then 4 mL of chloroform was added

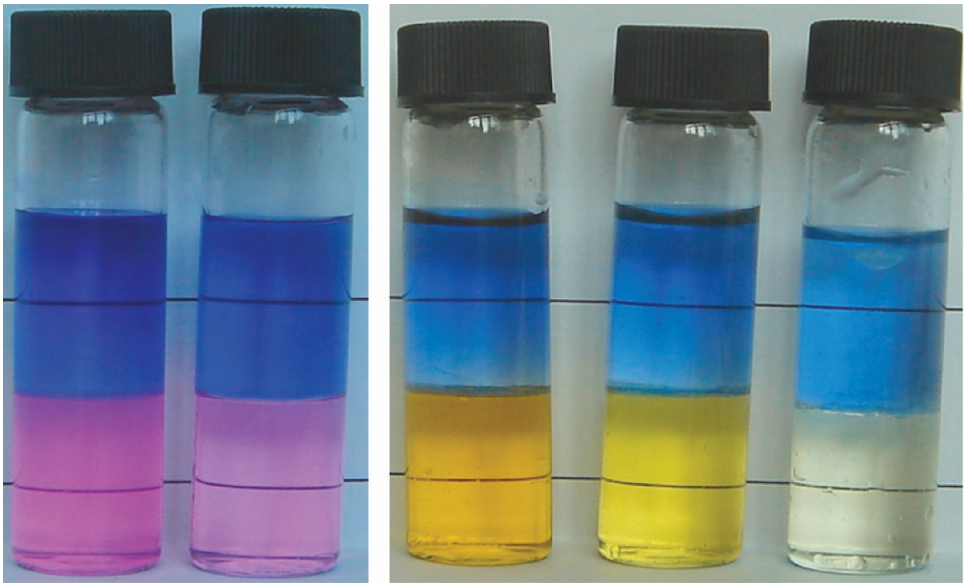

Figure 6. (Left) Upon the addition of CAM **1a** in chloroform to the aqueous mixture of MeB/RB (at different ratio) with shaking, the RB is completely transferred to the chloroform phase, while the MeB keeps intact in the aqueous phase. (Right) Upon the addition of **1a** in chloroform to the aqueous mixture of MeB/MO (at different ratio) with shaking, the MO is completely transferred to the chloroform phase, while the MeB keeps intact in the aqueous phase. **1a** can be replaced by **1b**−**1f**, **2b** and similar results are obtained, but **3d** tends to cause precipitation of the dye. General condition: $[CAM] = 1 \times 10^{-6}$ M.

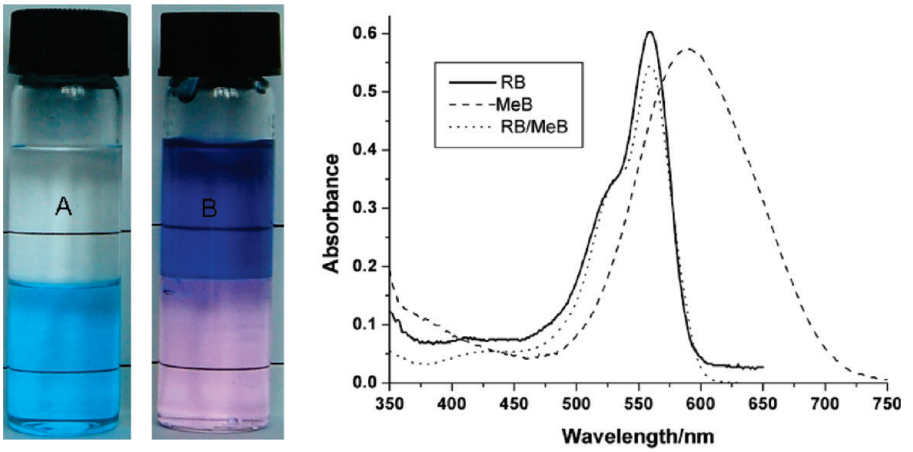

Figure 7. (Left) MeB in water can be completely transferred to the oil by **4d** (A), while for the mixture of RB/MeB, RB is almost exclusively transferred to the oil when an appropriate amount of **4d** is used (B). (Right) UV/vis spectra of RB alone, MeB alone transferred to oil, and of the dye transferred to oil from the aqueous mixture of RB/MeB, where nearly 100% separation of RB from MeB is found.

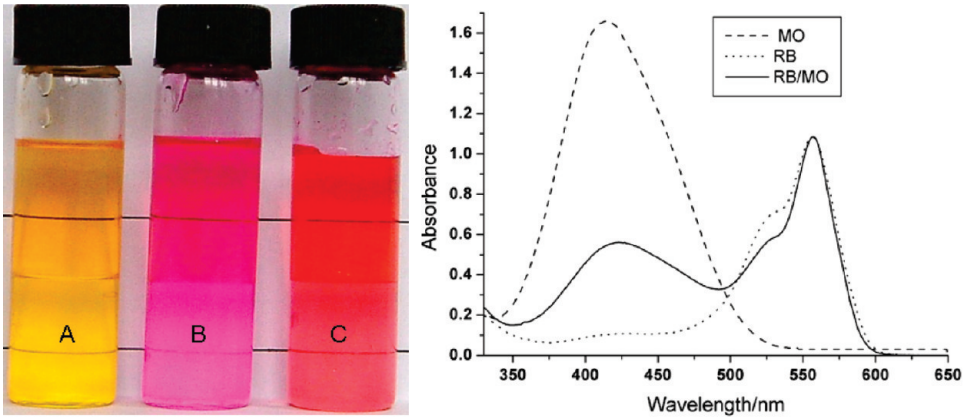

Figure 8. Either MO alone (A) or RB alone (B) in water can be transferred to the oil upon the addition of **1a** in chloroform, and for aqueous MO/RB, both are transferred to the oil (C). [MO] = [RB] and $[MO] + [RB] = 10^{-4}$ M, $[\mathbf{1a}] = 2.4 \times 10^{-6}$ M.

and the mixture was kept under stirring for another 2 days. After the solvents were removed on a rotary evaporator, the residue was dissolved in chloroform and dialyzed against chloroform (Spectro/Por, MWCO 2000) for 3 days. A white solid (10.82 g, 91%) was obtained after removal of the chloroform on a rotary evaporator. ^{1}H NMR analysis of the sample showed 90% of the amine protons were alkylated (M_n(calcd) = 74900).

4d was synthesized as follows: a mixture of **1d** (1.05 g, 0.033 mmol) and glycidol (0.5 g, 6.8 mmol) in chloroform (20 mL) wad stirred at 40 °C for 3 days, the solution was subjected to dialysis against chloroform for 2 days, removal of the solvent yields 1.45 g (100%) white solid. ^{1}H NMR (δ/ppm): 0.90 (t), 1.28 (s), 1.57 (t), 2−3 (broad, $CH_2CH_2NCH_2$), 3−4.5 (m, =$CHOH$, and CH_2OH).

2d, **3d**, and **5d** were synthesized similar to a previous process.[21]

Measurements. UV/vis spectra were recorded on a 760 CRT UV/vis spectrometer. ^{1}H NMR spectra were recorded on Bruker (600 MHz), with TMS as reference. Dynamic light scattering (DLS) was recorded on a commercial laser light scattering (LLS) spectrometer (Malvern Autosizer 4700) equipped with a solid-state laser (ILT 5500QSL, output power 100 mW at $\lambda 0$ = 532 nm) as the light source. All the DLS measurements were performed at 25 ± 0.1 °C. Size and polydispersity index ($\mu^2/\langle\Gamma\rangle^2$) were obtained by a CONTIN analysis mode. All the solutions at different concentrations were clarified using a 0.45 μm Millipore filter before the measurements.

Table 4. Dependence of MOs and RBs Transferred to the Oil on Both the Guest Ratio in Feed and the CAM Structure [a]

MO/RB/**1a** × 10^6/M in feed	MOs/RBs transferred to oil per CAM
1000/100/2	79.6/22
100/100/2	19.4/20
100/100/2 (**1b**)	4.6/11 (**1b**)
20/100/2	4.9/12

[a] Liquid−liquid transfer in water/chloroform biphasic mixture.

Dye Encapsulation. Typically, an aqueous solution of MO (4 mL, at concentration of 4×10^{-6} mol/L) and a chloroform solution of **1d** (4 mL, 1×10^{-6} M) were charged in a vial, after rigorous shaking, the mixture is put aside for phase balancing (3−7 days until each layer is clear) in a dark place. The chloroform layer was separated for a UV/vis measurement. Similarly, a diversity of samples were prepared with the concentration of MO varied while the concentration of **1d** set at a specified value.

Single-dye encapsulation was carried out similarly by mixing aqueous single-dye solution with the chloroform solution of the CAM. Double-dye encapsulation was carried out just by replacing the aqueous single-dye with aqueous double-dye solution in the similar process.

When the UV/vis absorbance is larger than 1, the chloroform layer is diluted until the absorbance is within 1, while the measured value is amplified to an equivalent concentration.

Saturated encapsulation can be calculated by [concentration of dye]/[concentration of CAM] (mol/mol) at inflection point.

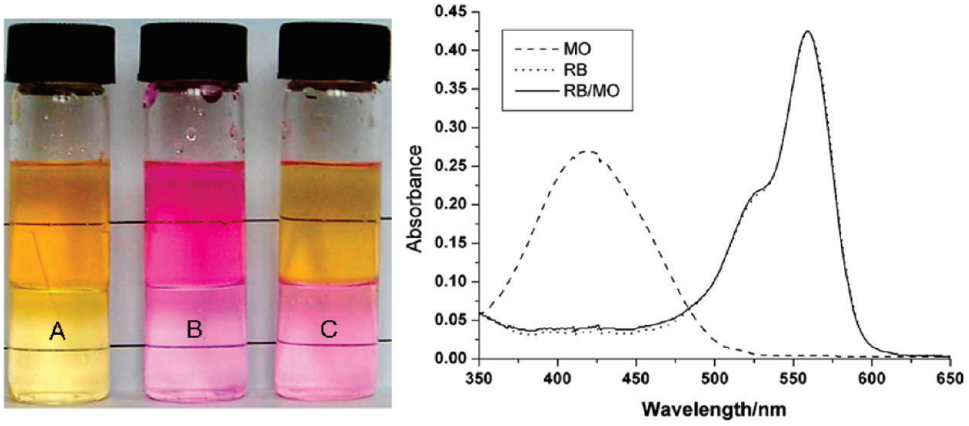

Figure 9. CAM **1f** can encapsulate either MO (A) or RB (B), but the mixture of MO/RB can be nearly 100% separated with certain amount of **1f** (C), as shown by the UV/vis spectra (right). Conditions: [**1f**] = 1×10^{-6} M. **1f** can be replaced by **2d** and similar behavior is found.

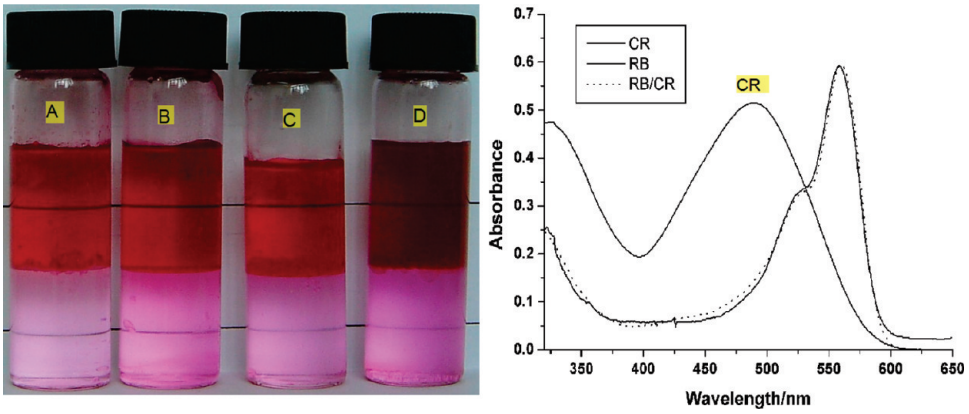

Figure 10. **1a**, **1b**, **1d**, and **2d** (A to D) are used to transfer the RB from the aqueous mixture of RB/CR to the oil, **1a**, **1b**, and **1d** are able to ~100% separate the mixture while **2d** is a little less efficient, as shown by the UV/vis spectra, where trace CR is detected in the oil (the spectra of pure CR is present here for reference).

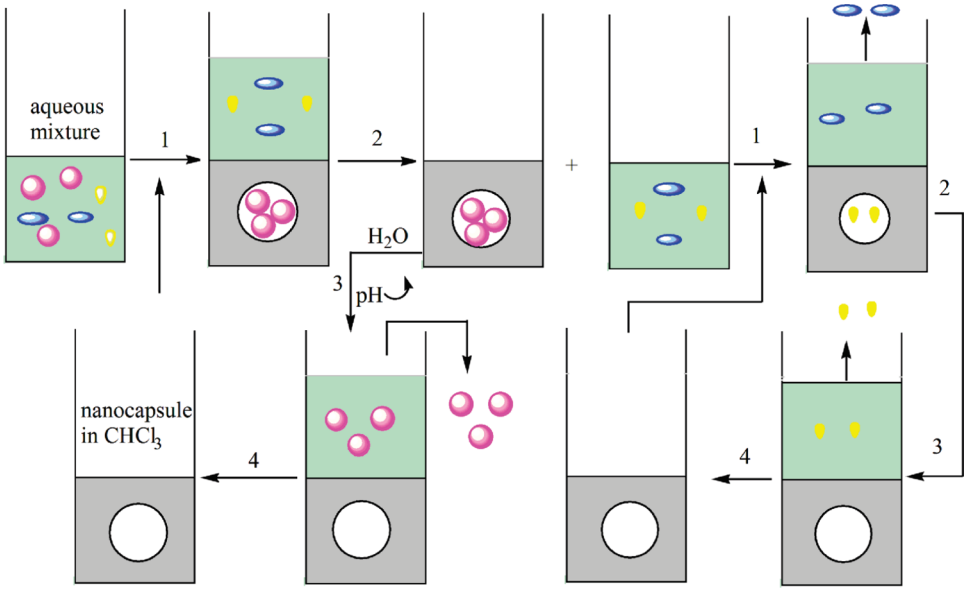

Figure 11. Illustration of the separation of ternary anionic mixture of RB/MO/MeB aided by CAM **1f** or **2d**. The magenta sphere represents RB, the yellow particle represents MO, and the blue particle represents MeB.

Acknowledgment. This work is supported by Shanghai Natural Foundation of China (No. 08ZR1420300) and Scientific Research Foundation for the Returned Overseas Chinese Scholars, State Education Ministry of China (0500241010).

References and Notes

(1) (a) Newkome, G. R.; Moorefield, C. N.; Baker, G. R.; Saunders, M. J.; Grossman, S. H. *Angew. Chem., Int. Ed.* **1991**, *30*, 1178–1180. (b) Baars, M. W. P. L.; Meijer, E. W. *Top. Curr. Chem.* **2000**, *210*, 131−182. (c) Zimmerman, S. C.; Lawless, L. J. *Top. Curr. Chem.* **2001**, *210*, 951−120. (d) Stiriba, S.-E.; Frey, H.; Haag, R. *Angew. Chem., Int. Ed.* **2002**, *41*, 1329–1334. (e) Satoh, T. *Soft Mater.* **2009**, *5*, 1972–1982.
(2) Hamilton, D. A; van Engen, D. *J. Am. Chem. Soc.* **1987**, *109*, 5035–5036.
(3) Pedersen, C. J. *J. Am. Chem. Soc.* **1967**, *89*, 2495.
(4) Gao, C.; Yan, D. Y. *Prog. Polym. Sci.* **2004**, *29*, 183–275.
(5) Stiriba, S. E.; Kautz, H.; Frey, H. *J. Am. Chem. Soc.* **2002**, *124*, 9698–9699.
(6) Schmaljohann, D.; Potschke, P.; Hassler, R.; Voit, B. I.; Froehling, P. E.; Mostert, B.; Loontjens, J. A. *Macromolecules* **1999**, *32*, 6333–6339.
(7) Garamus, V. M.; Maksimova, T. V.; Kautz, H.; Barriau, E.; Frey, H.; Schlotterbeck, U.; Mecking, S.; Richtering, W. *Macromolecules* **2004**, *37*, 8394–8399.
(8) Chen, Y.; Shen, Z.; Pastor-Perez, L.; Frey, H.; Stiriba, S. E. *Macromolecules* **2005**, *38*, 227–229.
(9) Liu, H. J.; Chen, Y.; Zhu, D. D.; Shen, Z.; Stiriba, S. E. *React. Funct. Polym.* **2007**, *67*, 383–395.
(10) Kramer, M.; Kopagzynska, M.; Krause, S.; Haag, R. *J. Polym. Sci., Part A: Polym. Chem.* **2007**, *45*, 2287–2303.
(11) Liu, C. H.; Gao, C.; Yan, D. Y. *Macromolecules* **2006**, *39*, 8102–8111.
(12) Kitajyo, Y.; Nawa, Y.; Tamaki, M.; Tani, H.; Takahashi, K.; Kaga, H.; Satoh, T.; Kakuchi, T. *Polymer* **2007**, *48*, 4683–4690.
(13) Hawker, C. J.; Chu, F. K. *Macromolecules* **1996**, *29*, 4370–4380.
(14) Radowski, M. R.; Shukla, A.; von Berlepsch, H.; Bottcher, C.; Pickaert, G.; Rehage, H.; Haag, R. *Angew. Chem., Int. Ed.* **2007**, *46*, 1265–1269.
(15) Xu, S. J.; Luo, Y.; Haag, R. *Macromol. Rapid Commun.* **2008**, *29*, 171–174.
(16) Tang, L. M.; Fang, Y.; Tang, X. L. *J. Polym. Sci., Part A: Polym. Chem.* **2005**, *43*, 2921–2930.
(17) Lin, Y.; Liu, X. H.; Dong, Z. M.; Li, B. X.; Chen, X. S.; Li, Y. S. *Biomacromolecules* **2008**, *9*, 2629–2636.
(18) Ren, Y.; Wang, G. W.; Huang, J. L. *Biomacromolecules* **2007**, *8*, 1873–1880.
(19) Liu, C. H.; Gao, C.; Yan, D. Y. *Angew. Chem., Int. Ed.* **2007**, *46*, 4128–4131.
(20) Wu, J. Y.; Liu, C. H.; Gao, C. *Open Macromol. J.* **2009**, *3*, 12–26.
(21) Wan, D. C.; Pu, H. T.; Cai, X. Y. *Macromolecules* **2008**, *41*, 7787–7789.
(22) Wan, D. C.; Yuan, J. J.; Pu, H. T. *Macromolecules* **2009**, *42*, 1533–1540.
(23) Baars, M. W. P. L.; Froehling, P. E.; Meijer, E. W. *Chem. Commun.* **1997**, 1959–1960.
(24) Frechet, J. M. J.; Tomalia, D. A. *Dendrimers and Other Dendritic Polymers*; Wiley: West Sussex, U.K., 2001.